Corona Loss Calculation for Unconventional High Surge Impedance Loading Transmission Lines

Mushfiqul Abedin Khan and Mona Ghassemi
Zero Emission, Realization of Optimized Energy Systems (ZEROES) Laboratory
Department of Electrical and Computer Engineering, The University of Texas at Dallas, Richardson, TX, USA
mushfiqul.abedinkhan@utdallas.edu, mona.ghassemi@utdallas.edu

***Abstract*—Corona effects are one of the most important factors to take into consideration when designing an overhead transmission line. Corona discharges cause power loss which should be considered during transmission line design. Unconventional high surge impedance loading (HSIL) lines have subconductors placed anywhere in space and have no bundle symmetry. They have the potential to produce greater natural power than conventional lines and conventional HSIL lines. This paper calculates corona loss in both fair and foul weather conditions for an envisaged unconventional HSIL line. It is seen that the unconventional lines under discussion undergo much greater corona loss than the conventional lines and conventional HSIL lines.**

Keywords— Corona loss, unconventional HSIL lines, transmission lines, overhead lines, high surge impedance loading, natural power.

2023 North American Power Symposium (NAPS) | 979-8-3503-1509-7/23/$31.00 ©2023 IEEE | DOI: 10.1109/NAPS58826.2023.10318608

I. Introduction

Corona discharges in the air are caused by the partial breakdown of air around high-voltage conductors, resulting in power loss. The yearly average corona loss is approximately 2 kW/km to 10 kW/km for 400 km conventional lines, and 20-40 kW/km for 800 km conventional lines, since longer lines typically require higher voltage [1]. Overall, the yearly corona loss under full load is equivalent to almost 10% of the resistive line losses, which rises when considering load factors of 60 to 70% [1]. Corona loss must be compensated for by the generation sector, especially during bad weather (rainy, snowy) when corona losses rise to much higher values.

The load flow pattern of some lines has changed significantly as a result of deregulation, uncoordinated long-term planning for expansion of the generation and transmission sectors, and the inclusion of renewable resources in some places, resulting in some lines being overloaded and others working below capacity. With these factors coupled with delayed investments in the transmission sector due to deregulation, the U.S. power system is very close to reaching its maximum loadability and stability margins [2-4]. A recent study has also shown that to reach net-zero emissions in America by 2050, the transmission capacity has to increase by about 60% by 2030 and triple by 2050, to connect further wind and solar energy resources to the US power grid [5].

Considering the restrictions and targets mentioned above, it is necessary to increase transmission lines' power delivery capabilities. HVDC transmission does exist as an option, but HVDC circuit breakers (CBs) have not been commercially available yet. Therefore, the power delivery capability of EHV AC transmission lines must be increased. This goal has traditionally been achieved by incorporating capacitor banks in series and shunt, which can decrease line reactance and inject reactive power, respectively. This results in increased transient stability and voltage-drop limits. However, this solution would be costly [2].

High surge impedance loading (HSIL) lines can be used to increase natural power [2]. HSIL line designs can be divided into conventional HSIL lines and unconventional HSIL lines. An unconventional HSIL line has an irregular arrangement of bundled subconductors in space as opposed to conventional HSIL lines that place subconductors symmetrically on circles. To realize these new unconventional HSIL line designs, many design criteria would need to be met, including corona discharge effects such as corona losses. If the electric field on and around the surface of subconductors increases above a specific threshold value which is determined from the corona onset gradient, the effects of corona become greater than acceptable levels. As a result, it is crucial to calculate the surface electric field accurately. We accomplish this by employing the new method we presented in our other paper [6].

In this paper, the aim is to evaluate existing models and formulae for calculating corona loss to employ in overhead line designs with unconventional conductor configurations targeting higher SIL values.

II. Corona Loss Models

A. Corona Loss in Fair Weather

The fair-weather corona loss is much lower compared to the corona loss during rain, snowfall, or other bad weather conditions for most of the transmission lines rated above 230 kV. Over a year, however, the weather is mostly dominated by fair conditions. Therefore, in annual corona loss calculations, fair-weather corona loss might as well be of some significance.

For dry, smooth, and clean conductors, which may or may not be of stranded type, the corona loss during fair weather can be calculated by the following empirical formula introduced by F.K. Peek.

$$P = \frac{241 \times 10^{-5}}{\delta}(f + 25)\sqrt{\frac{r}{D}}\left(\frac{V}{\sqrt{3}} - 21.1 m \delta r \ln\left(\frac{D}{r}\right)\right)^2 \quad (1)$$

This work was supported in part by the National Science Foundation (NSF) under Award #2306098.

Authorized licensed use limited to: Univ of Texas at Dallas. Downloaded on July 19,2024 at 06:00:21 UTC from IEEE Xplore. Restrictions apply.

where P is the corona loss in kW per km, r is the conductor radius, D is the average phase spacing, f is the power frequency in Hz, δ is the relative air density, V is the line voltage in kV_{rms}, and m is a surface irregularity factor for the conductor. The lengths are in cm units. The surface irregularity factor, m, is the ratio of the corona onset gradient for the conductor in use to that for a smooth, cylindrical conductor of the same dimensions. The corona onset gradient is the surface electric field threshold above which corona discharges may occur. Generally, m lies between 0.75 to 0.85 for clean and stranded conductors. Scratched and nicked conductors may have m between 0.6 to 0.8. The value of m lies between 0.3 to 0.6 for conductors having water droplets, snow, ice, insects, or growing vegetable matter on their surface. It may further get reduced to 0.2 for extreme conditions such as the presence of grease, insects, and vegetable matter on conductors through tropical forests, or, uneven layers of soil forming on conductors due to the presence of soil and moisture in dry, off-shore regions. In an African country, despite generating power at full capacity, low power was available at the receiving end due to very high corona losses even in fair weather. It was found that the conductors in the transmission line which was going through a tropical forest had insects and vegetable matter traversing through its length due to the deposition of grease on the conductor surface [7]. In a 230 kV line near the coast in Peru, very high fair weather corona loss was also witnessed. During daytime, windy conditions caused soil, sand, and other organic matter to deposit on the conductor surface. Due to the moist conditions during the night, the soil stuck to the surface resulting in uneven layers of contamination on the conductors [8].

For cases where the field lies close to the corona onset voltage, as well as for conductors that are too small or too large, Eq. (1) provides inaccurate results. Peterson's empirical formula for calculating fair weather corona loss is not affected by such issues and is given by:

$$P = \frac{2.09 \times 10^{-5}}{\left[\log\left(\frac{D_{eq}}{r}\right)\right]^2} f V^2 F\left(\frac{E}{E_c}\right) \tag{2}$$

where P, r, V, f are all as before, D_{eq} is the geometric mean distance between phase conductors, and $F(E/E_c)$ is a function depending on the ratio of the maximum surface electric field to the corona onset. The corona onset gradient can be found as follows.

$$E_c = 21.1 m\delta\left[1 + \frac{0.301}{\sqrt{\delta r}}\right] \tag{3}$$

Eq. (2) provides accurate results for E/E_c having values close to 1.3 [9]. Note neither Eq. (1) nor Eq. (2) consider bundled conductors. To calculate fair weather corona loss for bundled conductors, the following formula by EDF can be considered.

$$P = P_0 r^{1.8}(N+6)^2 . 10^{7(E^*-0.7)} \tag{4}$$

here P is in W/m units, P_0 is 1.5×10^{-2} for new or contaminated conductors and 1.5×10^{-3} for aged or clean conductors, N is the number of subconductors in a bundle and E^* is the ratio of the maximum conductor surface gradient to the critical corona onset gradient, where both δ and m are 1.

For highly contaminated ACSR (Aluminum Conductor Steel Reinforced) conductors with diameters in the range of 2.59 to 4.60 cm, and for bundles with $N = 2$ having diameters in the range of 2.19 to 2.59 cm, and with m being between 0.2 to 0.8, the following empirical formulae were introduced in [8].

$$P = -59.8 + 42.5 \log E_m + 19.7 \log d - 21.9 \log m \tag{5a}$$

$$P = -71.7 + 46.7 \log E_m + 23.0 \log d - 33.2 \log m \tag{5b}$$

where Eq. (5a) is used for single conductors and Eq. (5b) for two conductor bundles. Here, P is calculated in dB relative to a power of 1 W/m. E_m is the maximum conductor surface gradient and is generally calculated using:

$$E_m = \frac{q}{2\pi\varepsilon_0}\frac{1}{r}\left[1 + \frac{(N-1)r}{R}\right] \tag{6}$$

where q is the charge per unit length for each subconductor, r is the subconductor radius, R is the bundle radius found using:

$$R = \frac{B}{2\sin\left(\frac{\pi}{N}\right)} \tag{7}$$

where B is the bundle spacing. However, Eq. (6) considers only the charges present in the subconductors in a single phase and ignores those in the other phases and the image conductors. Considering the charges ignored in Eq. (6), the maximum conductor surface gradient can be expressed as follows.

$$E_{1m} = \frac{V_m}{(P_{11} - 0.5P_{12} - 0.5P_{13})}\frac{1}{N}\frac{1}{r}\left[1 + \frac{(N-1)r}{R}\right] \tag{8a}$$

$$E_{2m} = \frac{V_m}{(P_{22} - 0.5P_{21} - 0.5P_{23})}\frac{1}{N}\frac{1}{r}\left[1 + \frac{(N-1)r}{R}\right] \tag{8b}$$

$$E_{1m} = \frac{V_m}{(P_{33} - 0.5P_{31} - 0.5P_{32})}\frac{1}{N}\frac{1}{r}\left[1 + \frac{(N-1)r}{R}\right] \tag{8c}$$

where V_m is the peak phase voltage and P_{ij} are Maxwell's Potential coefficients and are found by:

$$P_{ii} = \ln\frac{2y_i}{r_{eq}} \tag{9a}$$

$$P_{ij} = P_{ji} = \ln\frac{\sqrt{(x_i - x_j)^2 + (y_i + y_j)^2}}{\sqrt{(x_i - x_j)^2 + (y_i - y_j)^2}} \tag{9b}$$

where r_{eq} is the equivalent conductor radius, and $i, j = 1,2,3\ and\ i \neq j$. The distances labeled x are the horizontal distances from the phases and the image conductors to a

Authorized licensed use limited to: Univ of Texas at Dallas. Downloaded on July 19,2024 at 06:00:21 UTC from IEEE Xplore. Restrictions apply.

reference vertical line and y represents the height of the phases and the image conductors. We can find r_{eq} as follows.

$$r_{eq} = R\left(\frac{Nr}{R}\right)^{\frac{1}{N}} \tag{10}$$

B. Corona Loss in Foul Weather

Corona discharge is significantly more damaging in terms of losses in bad weather conditions. Be it rain, snow, or hoarfrost, each one causes corona losses more than the one before. During foggy or humid conditions, condensation leads to water droplets forming around the conductor surfaces. Raindrops can also accumulate by precipitation. For each of the cases, an uneven layer of water forms around the conductor surface since the deposited water droplets are more elongated near the bottom part of the conductors due to the gravitational force. Other than gravity, an electromechanical force also acts due to the electric field in which the conductors are present [10]. For hydrophobic conductors which repel water, the droplets form all around its surface, whereas for hydrophilic conductors which do not, more water deposits along the bottom surface. New conductors are generally of hydrophobic type as opposed to old ones which are of hydrophilic type. It is because of this phenomenon that new conductors undergo higher foul weather corona loss [11]. Precipitation can also occur due to snow, ice, hoarfrost, etc., the latter having the worst effect on performance. Snow can deposit in dry or wet form. The effect of wet snow is similar to raindrops. Dry snow on the other hand deposits on the conductor surface at low temperatures, reducing m and increasing corona loss [7]. Freezing rain may cause ice accretion on the conductor surface, also decreasing m. During hoarfrost, freezing of water vapor on the conductor surface occurs, which may result in corona losses almost 3 to 4 times that in heavy rainfall [12, 13].

For three-phase transmission lines rated between 400 and 700 kV, corona losses were measured for different weather conditions for project EHV [7]. The resulting empirical formula found is as follows.

$$P = P_{FW} + \left[\frac{V}{\sqrt{3}} J r^2 \ln(1 + KR)\right] \sum_{1}^{3N} E^5 \tag{11}$$

where P is corona loss and P_{FW} is the fair-weather corona loss in kW/mile, V is the line voltage in kV_{rms}, J is a loss current constant which has a value of 5.35×10^{-10} for 500 and 700 kV lines and 7.04×10^{-10} for 400 kV lines. R is the rain rate and K is a wetting coefficient and is equal to 10 if R is in mm/h. For rain rate values in in./h, K is equal to 254. E is the conductor surface voltage gradient for its underside in kV/cm peak.

In Eq. (11), P_{FW} is insignificant compared to the second part of the equation. Table I shows the fair-weather corona loss values for different configurations used in the EHV project [14].

The data in project EHV were collected considering experimental lines, and thus, Eq. (11) might only be valid within the specific range of voltages and rainfall levels considered. BPA used experimental data from full-scale test lines, brought the effect of different altitudes into consideration, and concluded the following empirical formula [7].

TABLE I. FAIR WEATHER CORONA LOSS IN PROJECT EHV

Rating (kV)	Configuration	Fair Weather Corona Loss, kW/3-phase Mile
500	2.32-inch diameter Special conductor	1-3
500	1.465-inch diameter Plover conductor	2-8
700	1.465-inch diameter Plover conductor	5-30

$$P(dB) = 14.2 + 65\log\frac{E_m}{18.8} + 40\log\frac{d}{3.51} + \\ + K_1\log\frac{N}{4} + K_2 + \frac{A}{300} \tag{12}$$

where P is considered in dB relative to a power loss of 1 W/m, K_1 is 13 for $N \leq 4$ and 19 for $N > 4$, A is the altitude, and K_2 varies with the rainfall rate, RR, in the following way.

$$K_2 = 10\log\frac{RR}{1.676}, for\ RR \leq 3.6\ mm/h \tag{13a}$$

$$K_2 = 3.3 + 3.5\log\frac{RR}{3.6}, for\ RR > 3.6\ mm/h \tag{13b}$$

The corona loss found in dB from Eq. (12) can be converted to kW/mile by taking its antilog and bringing in a factor of 1.60934. Fair-weather corona loss can also be estimated by subtracting 17 dB from the mean corona loss in rain from each phase as per BPA. Since only one phase is considered in Eq. (12), to find the corona loss from a three-phase line, a multiple of three has to be included. Therefore, the corona loss in rain and fair weather can be found using:

$$P = 1.60934 \times 3 \times 10^{\frac{14.2+65\log\frac{E_m}{18.8}+40\log\frac{d}{3.51}+K_1\log\frac{N}{4}+K_2+\frac{A}{300}}{10}} \tag{14a}$$

$$P_{FW} = 1.60934 \times 3 \times 10^{\frac{mean\left(14.2+65\log\frac{E_m}{18.8}+40\log\frac{d}{3.51}+K_1\log\frac{N}{4}+K_2+\frac{A}{300}\right)-17}{10}} \tag{14b}$$

As of yet, no accurate empirical relationship has been developed for corona loss due to snow. As suggested in [7], equivalent rainfall rates have been considered as an alternative. 2.5 mm/h rate of rain can be considered for heavy snow, 0.6 mm/h rain rate for medium snow, and 0.1 mm/h for light snow respectively. For wet snow, a further loss multiplier of 2 is considered.

III. CASE STUDIES AND RESULTS

A. Conventional 500-kV Three Phase Transmission Line

The conventional 500 kV, 3-phase transmission line shown in Fig. 1 [15] has been considered to be the base case for our study. Each of the phases has 4 subconductors, each having a diameter of 26.82 mm. The subconductors are placed at the vertices of a square having a side of 45 cm. The phases were arranged horizontally with each phase at a distance of 12.3 m from the next, and all at a height of 28 m.

To find the fair-weather corona loss for this line, we must consider the bundled subconductors. Since Eqs. (1), (2), and (5a) do not involve the number of subconductors in each bundle, and

Authorized licensed use limited to: Univ of Texas at Dallas. Downloaded on July 19,2024 at 06:00:21 UTC from IEEE Xplore. Restrictions apply.

Eq. (5b) only considers bundles with two subconductors, only Eq. (4) can lead to an accurate result. It is also seen later that subtracting 17 dB from the mean corona loss due to rain found using the empirical formula by BPA can also provide an accurate estimate for the fair-weather corona loss for different altitudes. Table II shows the fair-weather corona losses in kW/3-phase mile found using Eqs. (4) and (14b).

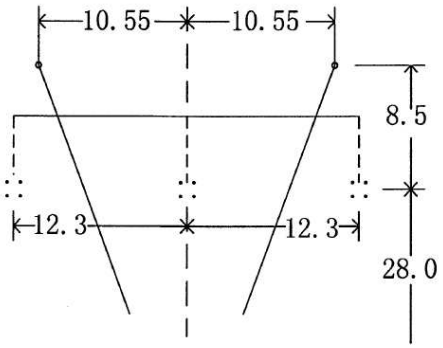

Fig. 1. The conventional 500 kV considered to be the base case.

TABLE II. FAIR WEATHER CORONA LOSS FOR THE CONVENTIONAL LINE

EDF, Eq. (4)	BPA, Eq. (14b)	
	A = 300 m	A = 1000 m
0.28	0.42	0.69

In [15], various compact lines with circular subconductor configurations were also discussed. In our study, we have considered these other configurations and compared the losses found with those for the conventional case. Table III shows the details of the configurations studied.

TABLE III. CONFIGURATIONS CONSIDERED IN [15]

Line Type	Bundle Configuration	Diameter of subconductors	Total aluminum cross section for each phase (mm^2)
Conventional	$4 \times (400/35) mm^2$	26.82	1600
Compact	$4 \times (400/50) mm^2$	27.63	1600
	$5 \times (300/40) mm^2$	23.94	1500
	$6 \times (240/40) mm^2$	21.66	1440
	$6 \times (240/30) mm^2$	21.60	1440

Fig. 2 shows the corona loss in rain for various rain rates for the conventional and the compact line with 4 subconductors using Eq. (11). It is seen in Fig. 2 that the compact line undergoes much greater corona loss in rain, which increases at a greater rate as the rainfall rate increases. The adjacent phases of the compact line are spaced only 6 m apart compared to the 12.3 m phase distance of the conventional line. This means that the surface electric field for the phase conductors in the compact line is much higher than that for the conventional line leading to much higher corona losses. Fig. 3 shows the comparison considering all the configurations from Table III. It is apparent from Fig. 3 that the compact lines all have greater corona loss in rain than the conventional line. As the number of subconductors is increased for the compact line, the corona loss decreases. It is noteworthy that for all the compact design configurations considered here, the bundle radius is kept the same as that of the conventional line, which is 31.82 cm. We also see that changing the steel cross-section from 40 mm^2 to 30 mm^2 has a negligible effect on the loss. Fig. 4 shows the corona loss in rain for the conventional line and the compact line with the 6-subconductor configuration with dimensions of (240/40) mm^2.

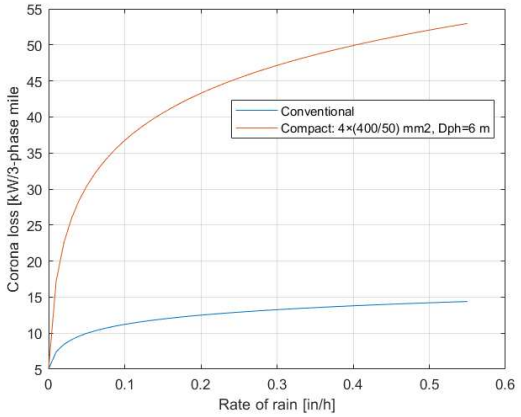

Fig. 2. Corona loss in rain for the conventional line and the 4×(400/50) mm^2 compact design.

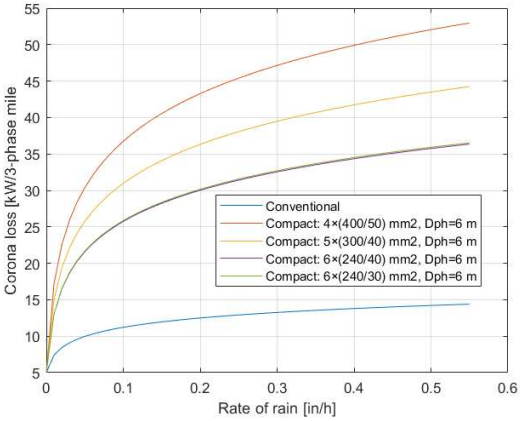

Fig. 3. Corona loss in rain for the line configurations presented in Table III.

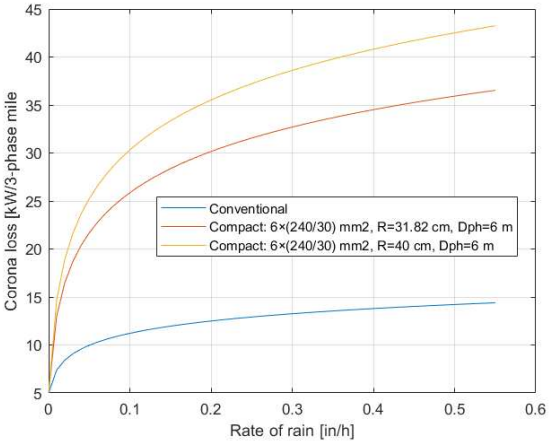

Fig. 4. Corona loss in rain for the conventional line and the 6×(240/30) mm^2 compact design for various bundle radii.

Authorized licensed use limited to: Univ of Texas at Dallas. Downloaded on July 19,2024 at 06:00:21 UTC from IEEE Xplore. Restrictions apply.

Fig. 4 shows that increasing the bundle radius from 31.82 cm to 40 cm causes the corona loss to increase provided that the phase distance remains constant. Since this causes the distance between subconductors of adjacent phases to decrease, their surface electric field increases, resulting in higher loss values. In Fig. 5, the same configurations are used keeping the bundle radius equal to 31.82 cm but varying the distance between adjacent phases.

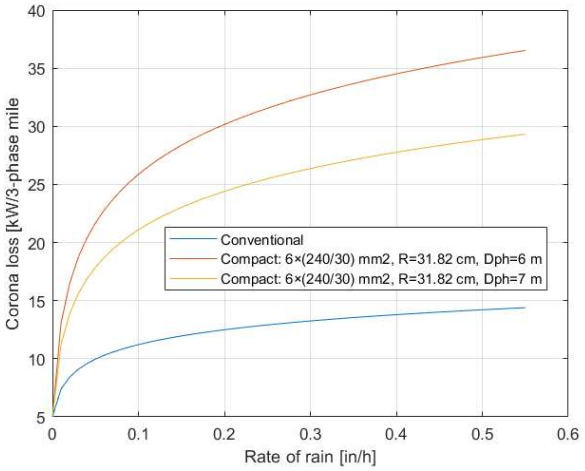

Fig. 5. Corona loss in rain for the conventional line and the 6×(240/30) mm^2 compact design for various phase gaps.

Increasing the phase gap from 6 m to 7 m helps reduce the surface electric field for the phase conductors, thus resulting in a reduction of the loss value. Fig. 6 shows the corona loss in rain for the conventional line for various altitudes via Eq. (14a).

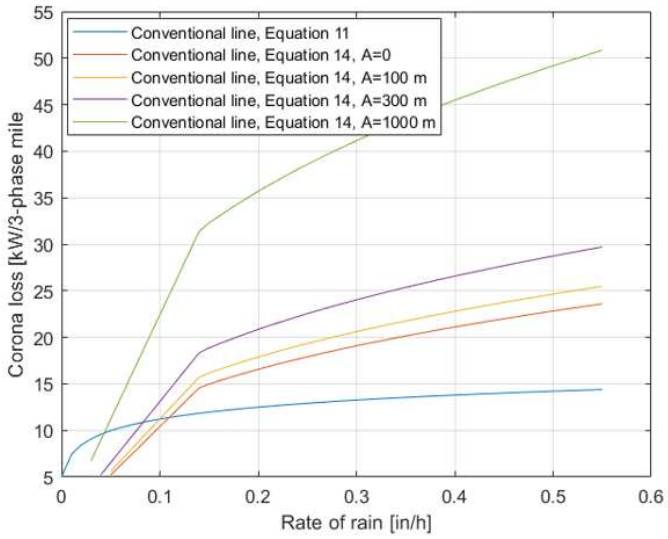

Fig. 6. Corona loss in rain for the conventional line using Eq. (14a).

B. An Unconventional 500-kV Three Phase Transmission Line with 8 Subconductors in Each Phase

Recently, we have proposed an unconventional 3-phase transmission line configuration consisting of 8 subconductors of diameter 20.93 mm per phase arranged in an inverted delta configuration [6]. The term unconventional here implies that the bundles do not have conventional symmetry. This new design proved to have a higher natural power compared to the conventional and compact designs previously discussed. Here, we have analyzed the corona loss in fair and foul weather for this newly proposed line. Fig. 7 shows the geometry of the unconventional three-phase transmission line.

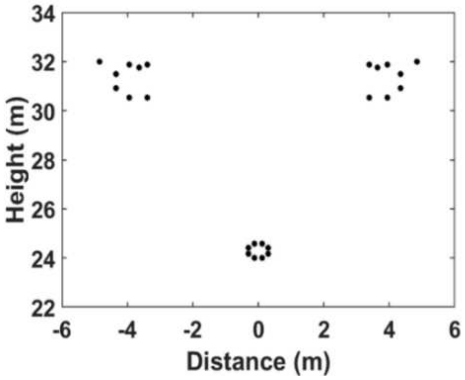

Fig. 7. Conductor configuration of the unconventional line with 8 subconductors.

Again, Eqs. (1), (2), (5a) and (5b) are not applicable to calculate the fair-weather corona loss for this line since the first three equations only work for single conductor phases, and Eq. (5b) only works for 2-conductor bundles. To find P_{FW}, Eqs. (4) and (14b) can be used. However, since this is an unconventional line, simply using Eqs. (8a), (8b), and (8c) would not lead to accurate E_m values. Recently, we have proposed a novel method to calculate surface electric field for unconventional lines [6]. Using this method to find E_m, the fair weather corona loss values in kW/3-phase mile will be as shown in Table IV.

TABLE IV. FAIR WEATHER CORONA LOSS FOR THE UNCONVENTIONAL LINE

EDF, Eq. (4)	BPA, Eq. (14b)	
	A = 300 m	A = 1000 m
2.48	2.33	3.99

The same E_m values for each phase are then used in Eq. (11) and Eq. (14a) to find the corona loss against rainfall rate. Figs. 8 and 9 show the resulting plots respectively.

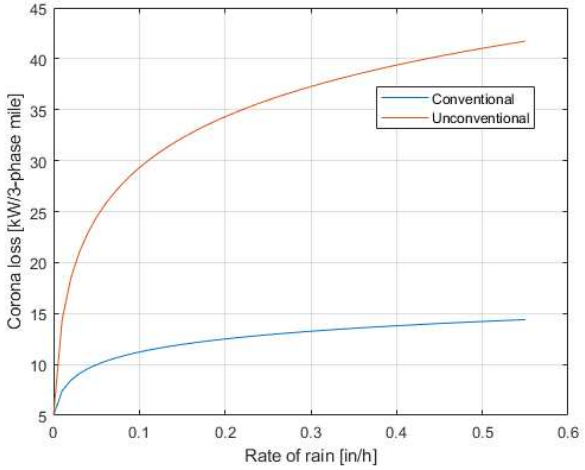

Fig. 8. Corona loss in rain for the conventional and the unconventional lines found using Eq. (11).

Authorized licensed use limited to: Univ of Texas at Dallas. Downloaded on July 19,2024 at 06:00:21 UTC from IEEE Xplore. Restrictions apply.

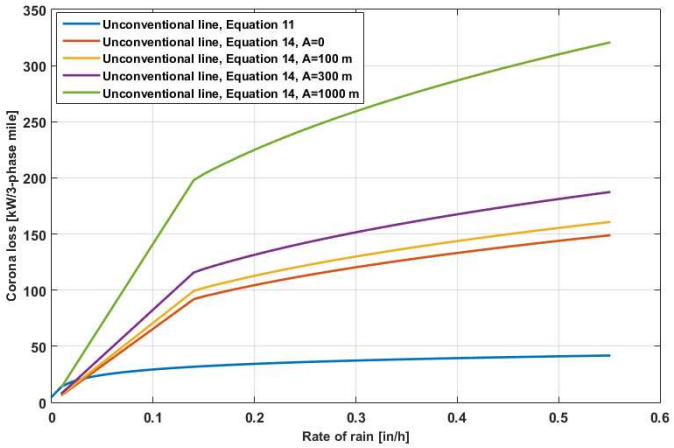

Fig. 9. Corona loss in rain for the unconventional line for various altitudes.

Further studies on unconventional HSIL lines and their combination with TEP can be found in our other papers [16-22]. Among the difficulties of designing HSIL lines, live line working may be challenging due to the interaction of maintenance personnel and those compact lines with unconventional bundle arrangements especially in freezing conditions [23-27], that has not been studied yet.

IV. Conclusion

In this paper, we have discussed the various methods of calculating corona loss in both fair and foul weather conditions. From the calculations, it can be seen the dependence of corona loss on parameters such as the bundle radius, the distance between adjacent phases, the number of subconductors in bundled conductors, and the altitude above sea level. As a result of the calculations, the unconventional HSIL lines envisioned in this paper will have more corona loss.

References

[1] R. D. Begamudre, *Extra High Voltage AC Transmission Engineering,* Tunbridge Wells, Kent, UK: New Academic Science Limited, 2013.

[2] M. Ghassemi, "High surge impedance loading (HSIL) lines: A review identifying opportunities, challenges, and future research needs," *IEEE Trans. Power Del*., vol. 34, no. 5, pp. 1909–1924, 2019.

[3] J. Hernandez, J. Segundo, P.Gomez, M. Borghei, and M. Ghassemi, "Electromagnetic transient performance of optimally designed high surge impedance loading lines," *IEEE Power & Energy Soc. General Meeting (PESGM),* 2020, pp. 1-5.

[4] M. Borghei and M. Ghassemi, "Geometrically optimized phase configurations and sub-conductors in the bundle for power transmission efficiency," *IEEE Electr. Insul. Conf. (EIC)*, 2019, pp. 295-299.

[5] E. Larson, C. Greig, J. Jenkins, E. Mayfield, et al. "Net-Zero America: Potential pathways, infrastructure, and impacts," interim Rep., Princeton University, Princeton, NJ, December 2020. [Online]. Available: https://netzeroamerica.princeton.edu/img/Princeton_NZA_Interim_Report _15_Dec_2020_FINAL.pdf

[6] M. Abedin Khan and M. Ghassemi, "A new method for calculating electric field intensity on sub conductors in unconventional high voltage, high power density transmission lines," *IEEE Conf. Electr. Insul. & Dielectr. Phenomena (CEIDP)*, accepted.

[7] EPRI, *AC Transmission Line Reference Book-200 kV and Above*, Third Edition, 2005.

[8] E. Mombello, P. S. Maruvada, "Measurement and analysis of corona losses generated by heavily contaminated conductors", *International Symp. High Voltage Eng. (ISH)*, Bangalore, India, Aug. 2001.

[9] C. F. Wagner, E. L. Peterson and I. W. Gross, "Corona consideration on high-voltage lines and design features of Tidd 500 kV lines," *AIEE Trans. Power App. & Syst.,* vol. 66, no. 1, pp. 1583-1591, 1947.

[10] W. N. English, "Corona from a water drop," *Phys. Rev.,* vol. 74, no. 2, pp. 179-189, 1948.

[11] P. S. Maruvada, "Corona transmission covering the subject from three types of lines," Eskom Holdings Limited, 2011.

[12] K. Lahti, M. Lahtinen, K. Nousiainen, "Transmission line corona losses under hoar frost conditions," *IEEE Trans. Power Del.,* vol. 12, no. 2, pp. 928-933, 1997.

[13] N. N. Tikhodeev, "Mitigation of corona losses on EHV overhead lines through voltage control," *Proc. St. Petersburg IEEE Chapter,* pp. 3-13, 2000.

[14] J. G. Anderson, M. Baretsky, and D. D. MacCarthy, "Corona loss characterization of EHV transmission lines based on project EHV research," *IEEE Trans. Power App. & Syst.,* vol. PAS-85, no. 12, pp. 1196-1212, 1966.

[15] H. Wei-Gang, "Study on conductor configuration of 500-kV chang-fang compact line", *IEEE Trans. Power Del.,* vol. 18, no. 3, pp. 1002-1008, Jul. 2003.

[16] M. Abedin Khan and M. Ghassemi, "Calculation of audible noise and radio interference for unconventional high surge impedance loading (HSIL) transmission lines," *IEEE Conf. Electrical Insul. Dielectric Phenomena (CEIDP)*, East Rutherford, NJ, USA, 2023.

[17] M. Abedin Khan and M. Ghassemi, "Calculation of corona loss for unconventional high surge impedance loading (HSIL) transmission lines," *IEEE North American Power Symp. (NAPS)*, Asheville, NC, USA, 2023.

[18] B. Porkar, M. Ghassemi, and M. Abedin Khan, "Transmission expansion planning (TEP)-based unconventional high surge impedance loading (HSIL) line design concept," *IEEE North American Power Symp. (NAPS)*, Asheville, NC, USA, 2023.

[19] B. Dhamala and M. Ghassemi, "Transmission expansion planning via unconventional high surge impedance loading (HSIL) lines," *IEEE North American Power Symp. (NAPS)*, Asheville, NC, USA, 2023.

[20] B. Dhamala and M. Ghassemi, "A test system for transmission expansion planning studies meeting the operation requirements under normal condition as well as all single contingencies," *IEEE North American Power Symp. (NAPS)*, Asheville, NC, USA, 2023.

[21] B. Dhamala and M. Ghassemi, "A test system for transmission expansion planning studies for both normal condition and all single contingencies," *IEEE Open Access Journal of Power and Energy*, submitted for publication, 2023.

[22] B. Dhamala and M. Ghassemi, "Unconventional high surge impedance loading (HSIL) lines and transmission expansion planning," *IEEE North American Power Symp. (NAPS)*, Asheville, NC, USA, 2023.

[23] M. Ghassemi, M. Farzaneh, and W. A. Chisholm, "Three-dimensional FEM electrical field calculation for FRP hot stick during EHV live-line work," *IEEE Trans. Dielectr. Electr. Insul.*, vol. 21, no. 6, pp. 2531–2540, Dec. 2014.

[24] M. Ghassemi, M. Farzaneh, and W. A. Chisholm, "A coupled computational fluid dynamics and heat transfer model for accurate estimation of temperature increase of an ice-covered FRP live-line tool," *IEEE Trans. Dielectr. Electr. Insul.*, vol. 21, no. 6, pp. 2628–2633, Dec. 2014.

[25] M. Ghassemi and M. Farzaneh, "Coupled computational fluid dynamics and heat transfer modeling of the effects of wind speed and direction on temperature increase of an ice-covered FRP live-line tool," *IEEE Trans. Power Del.*, vol. 30, no. 5, pp. 2268–2275, Oct. 2015.

[26] M. Ghassemi and M. Farzaneh, "Effects of tower, phase conductors and shield wires on electrical field around FRP hot stick during live-line work," *IEEE Trans. Dielectr. Electr. Insul.*, vol. 22, no. 6, pp. 3413–3420, Dec. 2015.

[27] M. Ghassemi and M. Farzaneh, "Calculation of minimum approach distances for tools for live working under freezing conditions," *IEEE Trans. Dielectr. Electr. Insul.*, vol. 23, no. 2, pp. 987–994, Apr. 2016.

Authorized licensed use limited to: Univ of Texas at Dallas. Downloaded on July 19,2024 at 06:00:21 UTC from IEEE Xplore. Restrictions apply.